THE ASTROPHYSICAL JOURNAL, 565:L71–L74, 2002 February 1
© 2002. The American Astronomical Society. All rights reserved. Printed in U.S.A.

LARGE EQUIVALENT WIDTH Lyα LINE EMISSION AT $z = 4.5$: YOUNG GALAXIES IN A YOUNG UNIVERSE?

SANGEETA MALHOTRA[1,2,3] AND JAMES E. RHOADS[3]

Received 2001 November 2; accepted 2001 December 5; published 2002 January 11

ABSTRACT

The Large Area Lyman Alpha survey has found ≈150 Lyα emitters at $z = 4.5$. While stellar models predict a maximum Lyα equivalent width (EW) of 240 Å, 60% of the Lyα emitters have EWs exceeding this value. We attempt to model the observed EW distribution by combining stellar population models with an extrapolation of a Lyman break galaxy luminosity function at $z = 4$, incorporating observational selection effects and Malmquist bias. To reproduce the high EWs seen in the sample, we need to postulate a stellar initial mass function with an extreme slope of $\alpha = 0.5$ (instead of 2.35), zero-metallicity stars, or narrow-line active galactic nuclei (AGNs). Not all the high-EW sources can be AGNs without exceeding the X-ray background or postulating a very steep redshift evolution. Only 7.5%–15% of galaxies need to show Lyα emission to explain the observed number counts. This raises the possibility either that star formation in high-redshift galaxies is episodic or that the Lyα galaxies we are seeing are the youngest 7.5%–15% and that Lyα is strongly quenched by dust at about 10^7 yr of age.

Subject headings: cosmology: observations — galaxies: evolution — galaxies: formation — galaxies: general — galaxies: statistics

1. INTRODUCTION

Nascent galaxies undergoing their first major burst of star formation are expected to contain many hot, young, massive stars, which ionize interstellar gas. Under standard conditions (case B), about two Lyα photons are produced for every three ionizing photons from the stars. Thus, Lyα photons can be a prominent signpost of primordial galaxies in formation (Partridge & Peebles 1967, hereafter PP67).

Based on these predictions a number of surveys have been carried out for about three decades (see Pritchet 1994 for a review), with little success until recently. We have recently undertaken a Large Area Lyman Alpha (LALA) survey (Rhoads et al. 2000) to identify a large sample of Lyα-emitting galaxies at high redshift ($z = 4.5 \pm 0.1$) through narrowband imaging and so characterize empirically star and galaxy formation in the early universe. Both our survey (Rhoads et al. 2000) and other recent searches over smaller volumes (Cowie & Hu 1998; Hu, Cowie, & McMahon 1998; Kudritzki et al. 2000; Fynbo, Möller, & Thomsen 2001; Pentericci et al. 2001; Stiavelli et al. 2001) are indeed finding high-redshift Lyα sources, albeit factors of ~100 fainter than the early predictions (PP67).

The low luminosity of this line could be due to smaller masses of the sources or low star formation rates. The equivalent width (EW) of the Lyα line can also be used to distinguish between these two scenarios. However, this is complicated by several factors: ionizing flux depends on stellar metallicity; active galactic nuclei may contribute to the ionizing flux; and resonant scattering of the Lyα line can make it more sensitive to dust than the adjoining continuum, but (depending on clumping and winds in the interstellar medium) need not do so (Neufeld 1991; Kunth et al. 1998).

2. OBSERVATIONS AND EQUIVALENT WIDTHS

2.1. *Survey and Data Reduction*

An efficient search for Lyα emitters (and other emission-line galaxies) was started in 1998 using the CCD Mosaic Camera at the Kitt Peak National Observatory's 4 m Mayall telescope. The Mosaic camera has eight 2048 × 4096 chips in a 4 × 2 array comprising a 36′ × 36′ field of view. The final area covered by the LALA survey is 0.72 deg^2 in two MOSAIC fields centered at $14^h25^m57^s$, +35°32′ (2000.0) and 02°05′20″, −04°55′ (2000.0). Five overlapping narrowband filters of width FWHM ≈ 80 Å are used. The central wavelengths are 6559, 6611, 6650, 6692, and 6730 Å, giving a total redshift coverage $4.37 < z < 4.57$. This translates into a surveyed comoving volume of 7.4×10^5 comoving Mpc^3 per field for $H_0 = 70$ km s^{-1} Mpc^{-1}, $\Omega_M = 0.3$, and $\Omega_\Lambda = 0.7$.

In this Letter we report on the data from the spring field centered at $14^h25^m57^s$, +35°32′ (2000.0) since all the imaging on this field at $z \approx 4.5$ is complete. In about 6 hr per filter per field we achieve line detections of about 2×10^{-17} ergs cm^{-2} s^{-1}. The survey sensitivity varies with seeing. Broadband images of these fields in a custom B_w filter ($\lambda_0 = 4135$ Å, FWHM = 1278 Å) and the Johnson-Cousins R, I, and K bands were taken as part of the NOAO Deep Wide-Field Survey (NDWFS; Jannuzi & Dey 1999).

The images were reduced using the MSCRED package (Valdes & Tody 1998; Valdes 1998) in the IRAF environment (Tody 1986, 1993), together with assorted custom IRAF scripts. Details of the data reduction can be found in the paper by Rhoads et al. (2000). Catalogs were generated using the SExtractor package. Fluxes were measured in 2.″32 (9 pixel) diameter apertures, and colors were obtained using matched 2.″32 apertures in registered images that had been convolved to yield matched point-spread functions.

2.2. *Selection Criteria*

The candidates are selected in the narrow bands with a detection threshold of 5 σ, where σ is the rms noise determined locally. To reduce the number of foreground [O II] and [O III] interlopers, we set the minimum observed equivalent width, EW > 80 Å. Also, the narrowband flux density should exceed the broadband flux density at the 4 σ confidence level for a source to be selected as an emission-line source. All these criteria are designed to keep the numbers of false candidates down to an acceptable level (Rhoads 2000). An additional con-

[1] Johns Hopkins University, 3400 North Charles Street, Baltimore, MD 21218.
[2] Hubble Fellow.
[3] Space Telescope Science Institute, 3700 San Martin Drive, Baltimore, MD 21218.

dition that the sources not be detected in the *B*-band image guards against selecting low-redshift sources and is roughly equivalent to a photometric redshift. These criteria yield 157 $z = 4.5$ Lyα candidates in the three nonoverlapping filters Hα0, Hα8, and Hα16. This corresponds to a source density of 4000 deg^2 per unit redshift and agrees with previous studies (Hu et al. 1998; Kudritzki et al. 2000) within the uncertainties.

2.3. *Equivalent Width Calculation*

The EW is calculated using narrow- and broadband photometry. The observed EW is given by $\mathrm{EW}_o = F_{\mathrm{Ly}\alpha}/f_\lambda = (W_R N - W_N R)/(R - N)$, where $F_{\mathrm{Ly}\alpha}$ is the flux of the Lyα line, f_λ is the flux density of the continuum, W_N and W_R are widths of the *R* band (1568 Å) and the narrow band (80 Å), respectively, and *R* and *N* are the respective fluxes in the *R* band and the narrow band in which the source is detected.

The correction factor for intergalactic absorption is estimated using the prescription of Madau (1995). For the broad band, this is $\mathscr{A} = 0.58$–0.68 for $z = 4.57$–4.37. For a Lyα line that is symmetric about zero velocity, we find $\mathscr{A} = 0.64$. Thus, the two corrections approximately cancel. The rest-frame EW is then given by $\mathrm{EW} = \mathrm{EW}_o/(1 + z)$. The division by $(1 + z)$ corrects for Hubble expansion.

Figure 1 shows the cumulative distribution of the rest-frame EW. The continuum is not detected in approximately half the sources, and we use the actual measured *R* flux at the location of the narrowband source. This makes the EWs formally negative in many cases; they are then placed in the last bin of the histogram. The median of the distribution is 400 Å. Figure 1 also shows the cumulative distribution of EWs if we add 1 σ and 2 σ to the i-band flux, which gives some idea of the uncertainties in the measurement of the EW.

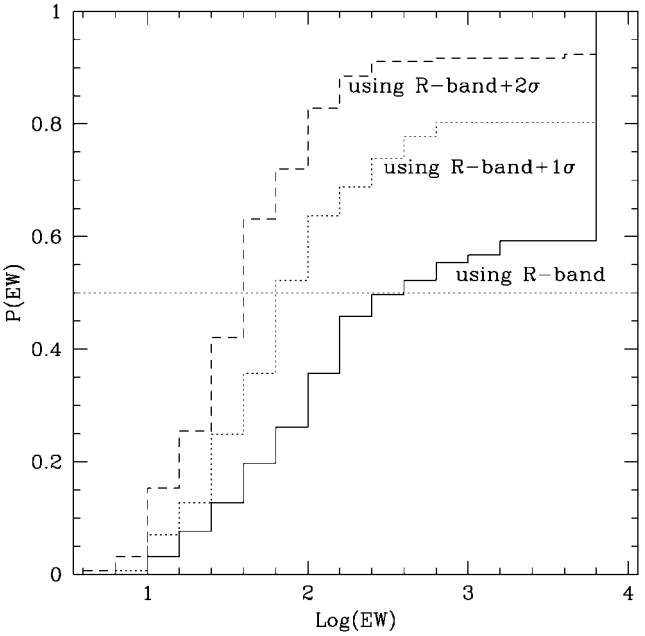


FIG. 1.—Cumulative distribution of Lyα EWs in the Lyα emitter sample. The *R*-band flux is not detected in about half of the sample. Measured *R*-band fluxes are used to calculate EWs (*solid line*), and sources with negative *R*-band fluxes are placed in the last bin. The dotted and dashed lines show the EWs calculated after adding 1 σ and 2 σ flux to the measured *R*-band flux. More than 60% of the sources show EWs greater than 240 Å, the maximum allowed by reasonable stellar population models (Charlot & Fall 1993).

3. MODELING THE DISTRIBUTION OF EQUIVALENT WIDTHS

The EW of the Lyα line from stellar systems depends on many factors: the fraction of ionizing photons absorbed by the gas, the dust content of the interstellar medium, and the relative numbers of ionizing and nonionizing photons in the UV. The last depends on the slope of the stellar initial mass function (IMF), the metallicity of the stellar population, and the age of the system. The presence of dust decreases the EW of the Lyα line, while metal-poor and more massive, young stars increase it. Charlot & Fall (1993) and Kudritzki et al. (2000) have calculated the Lyα EW for stellar populations with different properties.

Our approach here is to combine the luminosity function of galaxies at high redshift with stellar population models and simulate the observational biases reasonably to model the observed Lyα-emitter population. Since we have a reasonably large sample of Lyα emitters, we can use the distribution of EWs, as well as the total numbers of such objects, as constraints on the nature of these objects.

Three main elements go into modeling the observed number and distribution of EWs:

The luminosity function of galaxies at $z = 4.5$.—Since Lyα emitters are selected on the basis of a strong line, this sample can, and does, explore the faint end of the luminosity function (Fynbo et al. 2001); i.e., we can pick up objects with subdetection level continuum fluxes and bright emission lines. And as long as there are more faint sources than bright, selection on the basis of line luminosity will result in bias toward high-EW sources.

To model the effects of such biases and to explore the relation between line- and continuum-selected high-redshift sources, we use the luminosity function of Lyman break galaxies (LBGs) at $z = 4.0$, consistent with the faint-end luminosity function from the Hubble Deep Field (Pozzetti et al. 1998; Steidel et al. 1999). Translating the luminosity function to a cosmology with $H_0 = 70$, $\Omega_M = 0.3$, and $\Omega_\Lambda = 0.7$ at redshift $z = 4.5$, we get a Schecter function with $\phi_* = 1 \times 10^{-3}$ Mpc^{-3} mag^{-1}, $\alpha = -1.6$, and $M_* = 25.17$.

Stellar population modeling.—We estimate the EW of the Lyα line using the stellar population modeling program Starburst99 (Leitherer et al. 1999). For simplicity we consider three models: model A consists of continuous star formation with a Salpeter IMF ($\alpha = 2.35$), $Z = 1/20$ solar, and $M_{\mathrm{upper}} = 120\ M_\odot$. In model B we take the most extreme IMF we dare and set $\alpha = 0.5$. Model C consists of a zero-metallicity stellar population with an IMF slope of $\alpha = 2.35$, whose spectra at the age of 10^6 yr is derived by Tumlinson & Shull (2000). The shape of the age-EW distribution is assumed to be the same as for model A since $\alpha = 2.35$ is the same and since the shape of the age versus EW curve should depend mostly on the IMF slope α.

The continuum level at 1225 Å is given directly by the models. The line strength is derived by assuming that all the ionizing flux is absorbed by neutral hydrogen and produces two Lyα photons per three ionizing photons (case B). We assume that dust absorption and resonance scattering have no effect. All this maximizes the Lyα output from galaxies. The EW of Lyα is highest when the galaxies are young, and it asymptotically approaches a steady state value by age 10^7 yr, as seen in Figure 2 (see also Charlot & Fall 1993).

The Lyα EW distribution of the galaxy population is dependent on the age distribution. In this Letter we assume as our null hypothesis that the formation of galaxies at these epochs is continuous and uniform in time, which is to say that there is no special synchronization of galaxy formation better

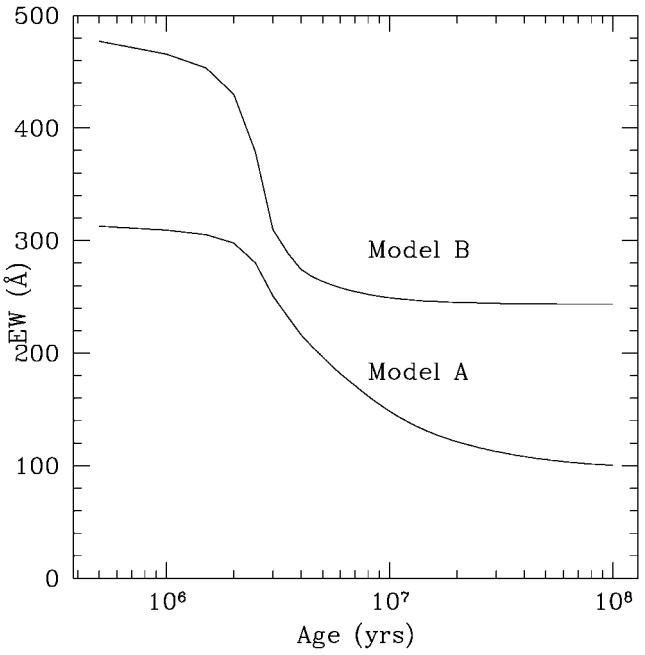


FIG. 2.—Evolution of the Lyα EW as a function of age for model A, where star formation is continuous with an IMF slope of 2.35, 1/20 solar metallicity, and an upper cutoff of 120 $M_{\odot}$. In model B the IMF slope is 0.5. Model C is derived from the zero-metallicity stellar populations of Tumlinson & Shull with an IMF slope 2.35 and is assumed to have a curve similar to model A, except that it is normalized to 1122 Å at age 10^6 yr (see text for details).

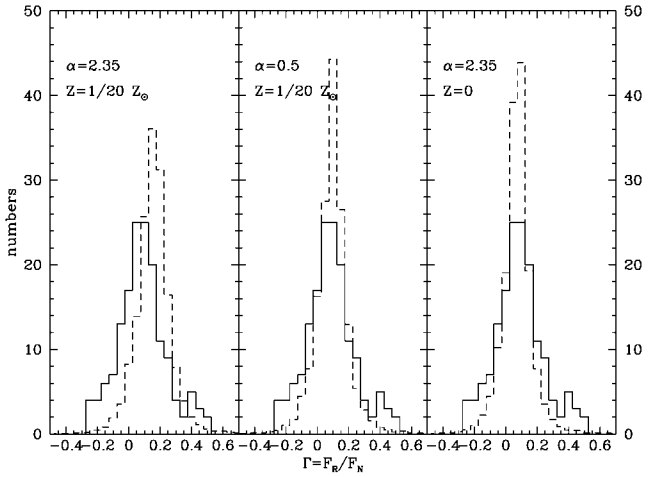


FIG. 3.—Observed distributions (*solid histograms*) and model distributions (*dashed histograms*) of the broadband-to-narrowband flux density ratio Γ are shown for models A, B, and C. The models' counts are normalized to match the observed numbers of Lyα sources. Corrections for intergalactic medium absorption have been applied to the modeled Γ-values. Models B and C fit better than model A, although none of the models can fully account for the high-Γ (i.e., low-EW) sources.

than 10^8 yr. The consequence of this assumption is that there should be 100 times as many galaxies of age 10^8 yr as 10^6 yr.[4] Therefore, the typical EW of the sample should be the EW of galaxies that are 10^8 yr old, with a tail extending to the highest EW for very young galaxies.

Observational selection effects.—Since objects are selected on the basis of having 5 σ flux in the narrow band and no restriction in the broadband, the error in EWs is dominated by the measurement errors in broadband flux. In about half the sample the continuum is undetected in the broadband *R* filter at 2 σ. An underestimate of the *R*-band flux can easily push up the EW estimates. So we model the effects of *R*-band measurement errors on the EW distribution.

Sky noise is the dominant source and is estimated by placing random apertures on the sky. We take the distribution of fluxes measured in 10^4 random apertures that satisfy one of the conditions of Lyα candidate selection, namely, that there be no detectable *Bw*-band flux. The distribution of fluxes in such apertures is then taken as the empirical distribution of errors in the *R*-band flux and shows higher tails than a Gaussian distribution.

The equivalent width (EW $= F_{\mathrm{Ly}\alpha}/f_{\lambda}$) is not the best formalism to model when the *R*-band continuum is not detected in half of the sources and when the flux density f_{λ} is unknown. Instead of modeling EWs, we work with the ratio of broadband-to-narrowband fluxes $\Gamma = f_{\lambda}(R)/f_{\lambda}(N)$. With the more uncertain (and small) quantity in the numerator instead of the denominator, the errors are much better behaved. Figure 3 shows the histogram of observed Γ versus calculated Γ in some of the models.

[4] We use the age distribution 0.5×10^6–10^8 yr. The upper limit is partly motivated by the age estimates of LBGs, whose luminosity function we use, and partly by the age of the universe, which is $\sim 10^9$ yr at $z = 4.5$.

Another advantage of this formalism is that in spite of the many elements that go into reproducing the Γ distribution, these elements are roughly separable in their effects on the distribution. With that in mind, we draw the following robust conclusions:

1. The total number of Lyα sources is dependent mostly on the luminosity function. We predict the total number of faint galaxies by extrapolating the LBG luminosity function to lower magnitudes. Only 7.5%–15% of these galaxies need to show Lyα emission to match the number of Lyα emitters found at $z = 4.5$.
2. The median of Γ is unaffected by the noise in *R*-band flux, which merely broadens the distribution of Γ. The median $\Gamma = 0.0814$, which corresponds to an EW of 430 in the Lyα line.
3. The width of the Γ distribution gives a measure of the scatter in the intrinsic value of Γ, as well as the flux errors in the *R* band. We find that the latter is the dominant contributor to the width of the distribution.

Figure 3 shows how the three models compare with the observed distribution of Γ. We see that none of the models fit perfectly. Model A clearly produces a higher Γ (lower EW) than observed and is most clearly disfavored. Models B and C reproduce the median Γ but do not fully account for the width of the distribution. The observed numbers of Lyα sources require that a fraction of faint galaxies show Lyα emission. This fraction is 15%, 8.5%, and 7.5% for models A, B, and C, respectively.

4. DISCUSSION AND CONCLUSIONS

With Lyα sources we are exploring the faint end of the luminosity function because selection on the basis of line luminosity pulls in sources not easily detected in the continuum (Fynbo et al. 2001). Are we also exploring the youngest set of galaxies by selecting them on the basis of their Lyα emission? In this Letter we have tried to answer that question by studying the EW distribution of these sources. The median EW of the population is too large to be explicable by ordinary stellar

populations. The distribution of EWs can be reasonably (though not perfectly) explained by postulating an IMF that favors more massive stars or a zero-metallicity population. Actually, metal-free gas is expected to produce stellar populations biased toward more massive stars (Bromm, Coppi, & Larson 2001a; Nakamura & Umemura 2001). The combined effect is to produce 10 times the ionizing flux compared to solar metallicity, Salpeter IMF populations (Bromm, Kudritzki, & Loeb 2001b). None of these scenarios can completely explain the low-EW tails of the distribution. These tails could be due to more evolved galaxies in which dust effects begin to be observable. Since the errors in *R*-band fluxes are responsible for much of the observed spread in EW, we need deeper *R*-band images to better see the real spread in EW.

The number of Lyα sources is 7.5%–15% of the numbers expected by extrapolating the luminosity function of LBGs. Perhaps this is a clue that we are only seeing the youngest galaxies, and therefore results are skewed toward high EWs of the Lyα line. Why then do we not see older galaxies with intermediate EWs in our sample? We are sensitive to EW $> 80/(1 + z)$. Perhaps dust formation after 10^7 yr quenches the Lyα line completely because of resonance scattering. In another possible scenario, perhaps the early star formation in galaxies is episodic, so we only see the galaxies when the star formation episode is less than 10^7 yr old. That is also when the galaxies are brighter. This scenario is also consistent with the blotchy appearances of high-redshift galaxies, if the different episodes happen in different parts of a galaxy (e.g., Colley et al. 1996).

The high EWs can also be a signature of quasar activity. If so, most of them have to be narrow-line quasars, otherwise we should see the Lyα line emission span more than one 80 Å filter. Some of the Lyα sources could be type II quasars, like the ones found by Norman et al. (2002) and Stern et al. (2002). *Chandra* Deep Field observations (Rosati et al. 2002) show that there are $\approx(2–3) \times 10^3$ X-ray sources per square degree at X-ray fluxes corresponding to the Lyα flux limit of our sample. (The X-ray–to–Lyα ratio is fixed using the Norman et al. 2002 object). Thus, if all the Lyα sources were type II quasars we would violate the X-ray background constraints by a factor of 4–5, unless there were no contribution to the X-ray background from redshifts $z < 4$ or $z > 5$. This is unphysical and contradicts the observed distribution of X-ray source redshifts: The *Chandra* Deep Field redshift distribution peaks at $z = 0.7–0.8$ and contains no $z > 4$ sources (Gilli et al., in preparation).

To conclude, this Letter reports on the EW distribution of Lyα-emitting galaxies at $z = 4.5$ and 5.7. The high median EW of the distribution requires that the galaxies be very young, have zero-metallicity, or a stellar IMF of slope $\alpha = 0.5$. AGNs can also produce high EWs. If so, we should be able to detect them with the current generation of X-ray observatories. High EWs observed in the large sample obtained by the LALA survey are harder to explain than individual objects (e.g., Ellis et al. 2001), and, therefore, pose questions that will help us understand galaxy and star formation in a young universe.

This work made use of images provided by NDWFS (Jannuzi & Dey 1999), which is supported by the National Optical Astronomy Observatory (NOAO). NOAO is operated by the Association of Universities for Research in Astronomy, Inc., under a cooperative agreement with the National Science Foundation. We thank Buell Jannuzi, Arjun Dey, and the rest of the NDWFS team for making their images public, and Richard Green and Jim De Veny for their support of the LALA survey. We thank Jason Tumlinson and Mike Shull for providing the zero -metallicity spectrum and Colin Norman and Tim Heckman for discussing a number of scenarios to explain these observations. Finally, we thank the referee for helpful comments. J. E. R.'s research is supported by an Institute Fellowship at the Space Telescope Science Institute (STScI). S. M.'s research funding is provided by NASA through Hubble Fellowship grant HF 01-111.01-98A from STScI. The STScI is operated by the Association of Universities for Research in Astronomy, Inc., under NASA contract NAS 5-26555.

REFERENCES

Bromm, V., Coppi, P. S., & Larson, R. 2001a, ApJ, 564, 23
Bromm, V., Kudritzki, R. P., & Loeb, A. 2001b, ApJ, 562, 464
Colley, W. N., Rhoads, J. E., Ostriker, J. P., & Spergel, D. N. 1996, ApJ, 473, L63
Cowie, L. L., & Hu, E. M. 1998, AJ, 115, 1319
Charlot, S., & Fall, S. M. 1993, ApJ, 415, 580
Ellis, R., et al. 2001, ApJ, 560, L119
Fynbo, J. U., Möller, P., & Thomsen, B. 2001, A&A, 374, 443
Hu, E. M., Cowie, L. L., & McMahon, R. G. 1998, ApJ, 502, L99
Jannuzi, B. T., & Dey, A. 1999, in ASP Conf. Ser. 191, Photometric Redshifts and High Redshift Galaxies, ed. R. J. Weymann, L. J. Storrie-Lombardi, M. Sawicki, & R. J. Brunner (San Francisco: ASP), 111
Kudritzki, R.-P., et al. 2000, ApJ, 536, 19
Kunth, D., Mas-Hesse, J. M., Terlevich, E., Terlevich, R., Lequeux, J., & Fall, S. M. 1998, A&A, 334, 11
Leitherer, C., et al. 1999, ApJS, 123, 3
Madau, P. 1995, ApJ, 441, 18
Nakamura, F., & Umemura, M. 2001, ApJ, 548, 19
Neufeld, D. A. 1991, ApJ, 370, L85
Norman, C., et al. 2002, ApJ, in press
Partridge, R. B., & Peebles, P. J. E. 1967, ApJ, 147, 868
Pentericci, L., et al. 2000, A&A, 361, L25
Pozzetti, L., Madau, P., Zamorani, G, Ferguson, H. C., & Bruzual A., G. 1998, MNRAS, 298, 1133
Pritchet, C. J. 1994, PASP, 106, 1052
Rhoads, J. E. 2000, PASP, 112, 703
Rhoads, J. E., Malhotra, S., Dey, A., Stern, D., Spinrad, H., & Jannuzi, B. T. 2000, ApJ, 545, L85
Rosati, P., et al. 2002, ApJ, 566, 667
Steidel, C. C., Adelberger, K. L., Giavalisco, M., Dickinson, M., & Pettini, M. 1999, ApJ, 519, 1
Stern, D., et al. 2002, ApJ, in press
Stiavelli, M., Scarlata, C., Panagia, N., Treu, T., Bertin, G., & Bertola, F. 2001, ApJ, 561, L37
Tody, D. 1986, Proc. SPIE, 627, 733
———. 1993, in ASP Conf. Ser. 52, Astronomical Data Analysis Software and Systems II, ed. R. J. Hanisch, R. J. V. Brissenden, & J. Barnes (San Francisco: ASP), 173
Tumlinson, J. & Shull, J. M. 2000, ApJ, 528, L65
Valdes, F. 1998, ASP Conf. Ser. 145, Astronomical Data Analysis Software and Systems VII, ed. R. Albrecht, R. N. Hook, & H. A. Bushouse (San Francisco: ASP), 53
Valdes, F., & Tody, G. 1998, Proc. SPIE, 3355, 497